EPJ Web of Conferences **137**, 09005 (2017) DOI: 10.1051/epjconf/201713709005
XIIth Quark Confinement & the Hadron Spectrum

Investigation of the low-energy kaons hadronic interactions in light nuclei by AMADEUS

K. Piscicchia[1,2,a], M. Cargnelli[3], C. Curceanu[1], R. Del Grande[1,4], L. Fabbietti[5,6], J. Marton[3], A. Scordo[1], D. Sirghi[1], I. Tucakovic[7], O. Vazquez Doce[5,6], S. Wycech[8], J. Zmeskal[3], G. Mandaglio[9,10], M. Martini[1,11], and P. Moskal[12]

[1] *INFN, Laboratori Nazionali di Frascati, 00044 Frascati, Italy*
[2] *Museo Storico della Fisica e Centro Studi e Ricerche Enrico Fermi, Italy*
[3] *Stefan-Meyer-Institut für Subatomare Physik, 1090 Wien, Austria*
[4] *Università degli Studi di Roma Tor Vergata, Rome, Italy*
[5] *Excellence Cluster 'Origin and Structure of the Universe', 85748 Garching, Germany*
[6] *Physik Department E12, Technische Universität München, 85748 Garching, Germany*
[7] *Ruđer Bošković Institute, Zagreb, Croatia*
[8] *National Centre for Nuclear Research, 00681 Warsaw, Poland*
[9] *Dipartimento M.I.F.T. dell'Università di Messina, 98166 Messina, Italy*
[10] *INFN Gruppo collegato di Messina, 98166 Messina, Italy*
[11] *Dipartimento di Scienze e Tecnologie applicate, Università 'Guglielmo Marconi', 00193 Roma, Italy*
[12] *Institute of Physics, Jagiellonian University, 30-059 Kracow, Poland*

Abstract. The AMADEUS experiment aims to provide unique quality data of K^- hadronic interactions with light nuclear targets, in order to solve fundamental open questions in the non-perturbative strangeness QCD sector, like the controversial nature of the $\Lambda(1405)$ state, the yield of hyperon formation below threshold, the yield and shape of multi-nucleon K^- absorption, processes which are intimately connected to the possible existence of exotic antikaon multi-nucleon clusters. AMADEUS takes advantage of the DAΦNE collider, which provides a unique source of monochromatic low-momentum kaons and exploits the KLOE detector as an active target, in order to obtain excellent acceptance and resolution data for K^- nuclear capture on H, ^{4}He, ^{9}Be and ^{12}C, both at-rest and in-flight.

1 Introduction

The AMADEUS (Anti-kaonic Matter At DAΦNE: An Experiment with Unraveling Spectroscopy) [1] experiment investigates the low-energy K^- hadronic interaction in light nuclei (e.g. H, ^{4}He, ^{9}Be and ^{12}C) in order to provide experimental constraints on the non-perturbative QCD in the strangeness sector. AMADEUS takes advantage of the low momentum (about 127 MeV/c), almost monochromatic, charged kaons provided by the decay of ϕ mesons at-rest at the DAΦNE factory [2]. The analyses presented here refers to the data acquired by the KLOE [3] collaboration during the 2004/2005 data taking campaign.

[a] e-mail: kristian.piscicchia@lnf.infn.it

When studying the low-energy QCD with u, d and s quarks the chiral perturbation theory is not applicable, due to the presence of the broad $\Lambda(1405)$ state just few MeV below the $\bar{K}N$ threshold. The $\Lambda(1405)$ is a $J^P = 1/2^-$ isospin $I = 0$ strange baryon resonance, assigned to the lowest $L = 1$ supermultiplet of the three-quark system, which decays into $(\Sigma\pi)^0$ through the strong interaction. Despite the fact that $\Lambda(1405)$ is a four-stars resonance in Particle Data Group (PDG) [4], its nature still remains an open issue. The three quark picture (uds) fails to reproduce the observed properties of this state. A review of the theoretical works, and references to the experimental literature can be found in [5]. According to the chiral unitary predictions [6] a high mass pole, coupled to the $\bar{K}N$ production channel and located around 1420 MeV, might contribute to the measured $\Lambda(1405)$ shape. The position of the $\Lambda(1405)$ clearly reflects the strength of the $\bar{K}N$ interaction, thus influencing the possible formation of $\bar{K}$ multi-nucleon bound states. For the di-baryonic kaonic bound state ppK^- theoretical predictions deliver a wide range of binding energies and widths [7] while the experimental results are contradictory [8–14]. Moreover, the extraction of ppK^- signal in K^- absorption experiments is strongly affected by the yield and the shape of the competing K^- double nucleon absorption (2NA) process. Similarly the shape of the $\Lambda(1405)$ state produced in K^-p absorption on bound protons, is distorted by the binding energy of the proton, as well as by the non-resonant $(\Sigma\pi)^0$ production below threshold. A key issue, which is addressed in the analyses described below, is then the search for a high mass pole of the $\Lambda(1405)$, exploiting in-flight K^- capture in light nuclear targets [15, 16] and the investigation of the corresponding non-resonant background.

In Section 2 the features of the DAΦNE accelerator and the KLOE detector are summarized. In Section 3 the event selection procedure is described. Sections 4 and 5 are dedicated to the obtained results, and ongoing analyses, regarding K^- multi-nucleon absorption processes, ppK^- states, resonant and non-resonant $Y\pi$ production in light nuclei.

2 The KLOE detector at DAΦNE

The AMADEUS experiment is conceived to integrate the high acceptance and momentum resolution KLOE detector with the low momentum K^- beam of the DAΦNE collider in a future dedicated setup. As a first step, the data collected by the KLOE collaboration during the 2004/2005 data taking, corresponding to $\sim 1.74\ \mathrm{fb}^{-1}$, were analysed. The KLOE detector was used as an active target, the hadronic interaction of negative kaons with the materials of the apparatus being investigated.

DAΦNE (Double Anular Φ-factory for Nice Experiments) is a double ring e^+e^- collider, designed to work at the center of mass energy of the ϕ particle; the ϕ meson decay produces charged kaons with low momentum ($\simeq$ 127 MeV/c) which allows to either stop them, or to explore the products of their low-energy nuclear absorptions.

The KLOE detector is centered around the interaction region of DAΦNE and is characterised by an acceptance of $\simeq 98\%$; it consists of a large cylindrical Drift Chamber (DC) [17] and a fine sampling lead-scintillating fibers calorimeter [18], all immersed in the axially simmetric magnetic field with intensity of 0.52 T, provided by a superconducting solenoid. The chamber is characterized by excellent position and momentum resolutions. Tracks are reconstructed with a resolution in the transverse $R - \phi$ plane $\sigma_{R\phi} \sim 200\,\mu$m and a resolution along the z-axis $\sigma_z \sim 2$ mm. The transverse momentum resolution for low momentum tracks ($(50 < p < 300)$MeV/c) is $\frac{\sigma_{p_T}}{p_T} \sim 0.4\%$. The calorimeter is composed of a cylindrical barrel and two endcaps, providing a solid angle coverage of 98%. The volume ratio (lead/fibers/glue=42:48:10) is optimized for a high light yield and a high efficiency for photons in the range (20-300) MeV/c. The photon detection efficiency is 99% for energies larger than 80 MeV and it falls to 80% at 20 MeV due to the cutoff introduced by the ADC and TDC thresholds. The position of the clusters along the fibers can be obtained with a resolution

$\sigma_{\parallel} \sim 1.4\,\mathrm{cm}/\sqrt{E(\mathrm{GeV})}$. The resolution in the orthogonal direction is $\sigma_{\perp} \sim 1.3\,\mathrm{cm}$. The energy and time resolutions for photon clusters are given by $\frac{\sigma_E}{E_\gamma} = \frac{0.057}{\sqrt{E_\gamma(\mathrm{GeV})}}$ and $\sigma_t = \frac{57\,\mathrm{ps}}{\sqrt{E_\gamma(\mathrm{GeV})}} \oplus 100$ ps.

The DC entrance wall composition is 750 μm of carbon fibre and 150 μm of aluminum foil. Dedicated GEANT Monte Carlo simulations of the KLOE apparatus show that out of the total number of kaons interacting in the DC entrance wall, about 81% are absorbed in the carbon fibre component and remaining 19% in the aluminum foil. The KLOE DC is filled with a mixture of helium and isobutane (90% in volume ^{4}He and 10% in volume C_4H_{10}).

Besides atomic K^- captures an important contribution of in-flight K^- nuclear absorptions, in different nuclear targets from the KLOE materials, was evidenced and characterised, enabling exploit the in-flight process to perform invariant mass spectroscopy [15].

3 Particle Identification

The investigation of the negatively charged kaons interactions in nuclear matter is performed through the reconstruction of hyperon-pion and hyperon-nucleon/nucleus correlated pairs productions, following the K^- absorptions in H, ^{4}He, ^{9}Be and ^{12}C. The $\Lambda(1116)$ identification proceeds through the reconstruction of the $\Lambda \rightarrow p + \pi^-$ (BR = 63.9 ±0.5%) decay vertex. A spatial resolution below 1 mm is achieved for vertices found inside the DC volume (evaluated with Monte Carlo simulations). The obtained $M_{p\pi^-}$ invariant mass mean value is 1115.753±0.002 MeV/c^2 (only statistical error is given, the systematics being under investigation), with a resolution of σ=0.5 MeV/c^2. The particle identification takes advantage of both dE/dx information from the DC wires and the measurement of the energy released in the Calorimeter, as described in [1]. The Λ decay radial vertex position (ρ_Λ), represented in fig. 1, shows the topology of the K^- absorptions in KLOE. Four components are distinguishable, from inside to outside we recognize K^- absorptions in the DAΦNE beryllium sphere ($\sim$ 5 cm), the DAΦNE aluminated beryllium pipe ($\sim$ 10 cm), the KLOE DC entrance wall (aluminated carbon fibre $\sim$ 25 cm) and the long tail originating from K^- interactions in the gas filling the KLOE DC (25-200 cm). Σ particles are identified through their decay into $\Lambda\gamma$ or pπ as reported in [15, 16]. The K^- absorption vertex position, between the hyperon and a correlated produced particle (pion, proton etc.) is then used to select the target. As an example, the obtained resolution on the radial coordinate ($\rho_{\Lambda p}$) for the Λp vertex is 1.2 mm. Cuts on the absorption vertex radial position were optimised, based on MC simulations and a study of the Λ decay path, to select the targets with minimal contamination from other components. More details on the particle identification procedure can be found in [19]

4 K^- absorption on two nucleons in the Σ^0p final state

In [19], a high purity sample of Σ^0p events, from K^- captures in the ^{12}C, was reconstructed. Σ^0p is (together with Λp) an expected decay channel of the ppK^- cluster, with the advantage to be free from the Σ N $\rightarrow$ Λ N' conversion processes. The conversions strongly affect the uncorrelated Λp production thus distorting the observed spectra.

A simultaneus fit of the: Σ^0p invariant mass, the relative angle of the Σ^0 and proton in the laboratory system $\cos(\theta_{\Sigma^0 p})$, the Σ^0 and the proton momenta was performed to the following simulated processes:

- $K^-A \rightarrow \Sigma^0 - (\pi)p_{spec}(A')$ (1NA),
- $K^-pp \rightarrow \Sigma^0 p$ (2NA),
- $K^-ppn \rightarrow \Sigma^0 pn$ (3NA),

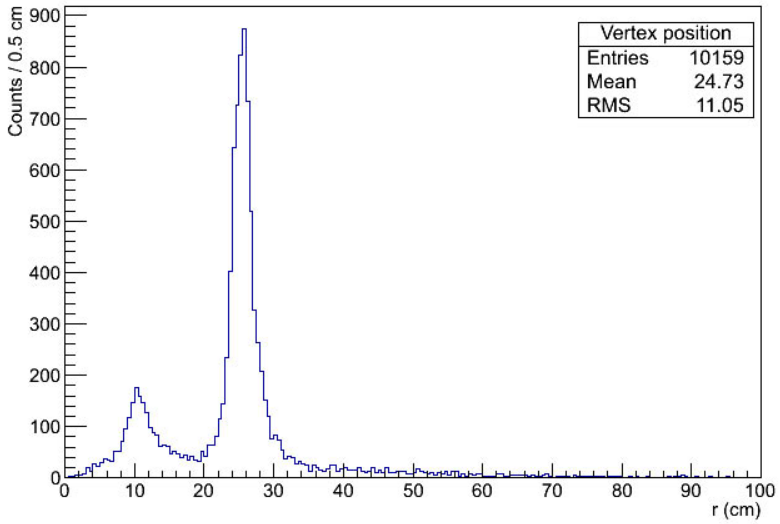

Figure 1. *Radial position distribution ρ_Λ, of the Λ decay vertex, for 2004-2005 KLOE collected data.*

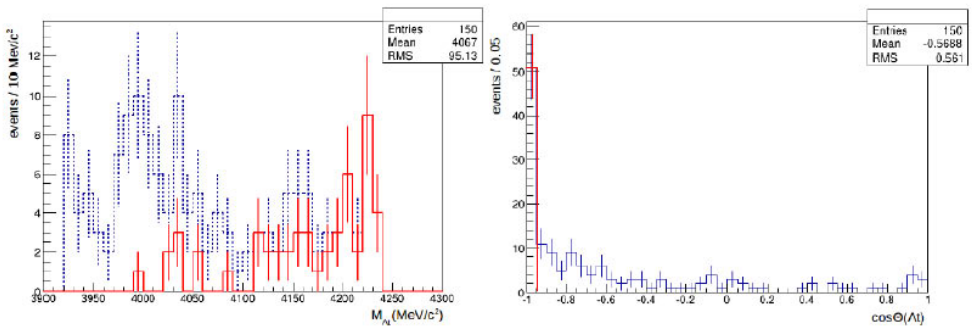

Figure 2. *(Colour online.) Λt invariant mass (left) and $cos\theta_{\Lambda t}$ (right). The events corresponding to the $cos\theta_{\Lambda t} < -0.95$ selection are shown in red.*

- $K^-ppnn \rightarrow \Sigma^0 pnn$ (4NA).

Also Final State Interactions (FSI) of the Σ^0 and p emerging from a K^-pp capture were taken into account.

The yield of the 2NA, when the produced Σ^0 and p particles are free form any FSI process, was measured for the first time, with good precision. More difficult is to disentangle the 3NA from 2NA + FSI processes due to their similar expected shapes. The obtained results are summarized in Table 4. A second fit was carried out including a ppK^- component, decaying into $\Sigma^0 p$. A systematic scan of possible binding energies and widths, varying within 15-75 MeV and 30-70 MeV respectively, was performed. The best fit resulted in a binding energy of 45 MeV and a width of 30 MeV. The resulting yield normalised to the number of stopped K^- is $ppK^-/K^-_{stop} = (0.044 \pm 0.009 stat^{+0.004}_{-0.005} syst) \times 10^{-2}$.

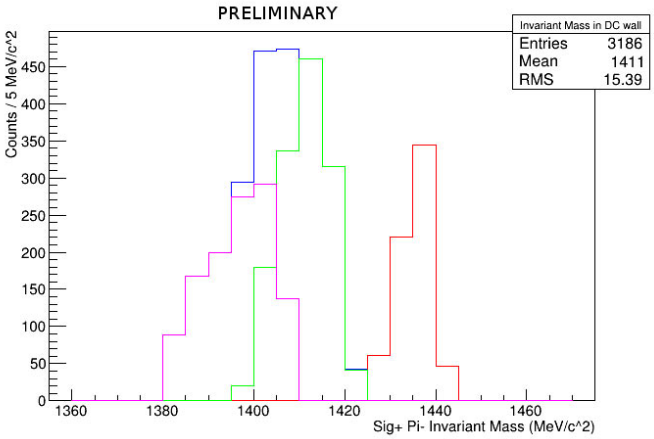

Figure 3. *(Colour online.) $m_{\Sigma\pi}$ invariant mass distributions in-flight (green) and at-rest (violet) in ^{12}C. Blue is the sum of green and violet curves. The red curve refers to K^- absorptions on Hydrogen*

The significance of the bound state with respect to a statistical fluctuation was checked by means of an F-test. The contribution of the ppK$^-$ component was found to be significant at the level of 1σ only. Although the measured spectra are compatible with the hypothesis of a ppK$^-$ contribution, the significance of the result is not sufficient to claim the discovery of the state. We refer to [19] for the details of the analysis.

Table 1. Production probability of the Σ^0p final state for different intermediate processes normalised to the number of stopped K$^-$ in the DC wall. The statistical and systematic errors are shown as well [19].

Process	yield / $K^-_{stop}\times10^{-2}$	$\sigma_{stat}\times10^{-2}$	$\sigma_{syst}\times10^{-2}$
2NA-QF	0.127	±0.019	$^{+0.004}_{-0.008}$
2NA-FSI	0.272	±0.028	$^{+0.022}_{-0.023}$
Tot 2NA	0.399	±0.033	$^{+0.023}_{-0.032}$
3NA	0.274	±0.069	$^{+0.044}_{-0.021}$
Tot 3 body	0.546	±0.074	$^{+0.048}_{-0.033}$
4NA + bkg.	0.773	±0.053	$^{+0.025}_{-0.076}$

The measurement of the, extremely rare, 4NA absorption process ($K^- + {}^4He \rightarrow \Lambda t$) is presently ongoing. To this aim K$^-$ captures in the gas filling the KLOE DC are exploited, with the goal to pin down the Λt 4NA production in ^{4}He. Some Λt events were identified in [20, 21] but the 4NA contribution was not extracted. In our work the highest statistics ever of correlated Λt production was evidenced (150 events). The preliminary Λt invariant mass and angular correlation distributions are shown in Fig. 2 left and right respectively.

The signature of K$^-$ 4NA in ^{4}He is the production of back-to-back Λt pairs, with the highest energy permitted by kinematics. Such events are represented in red in Fig. 2, and correspond to the cut $cos\theta_{\Lambda t} < -0.95$. The fit of the measured spectra is ongoing.

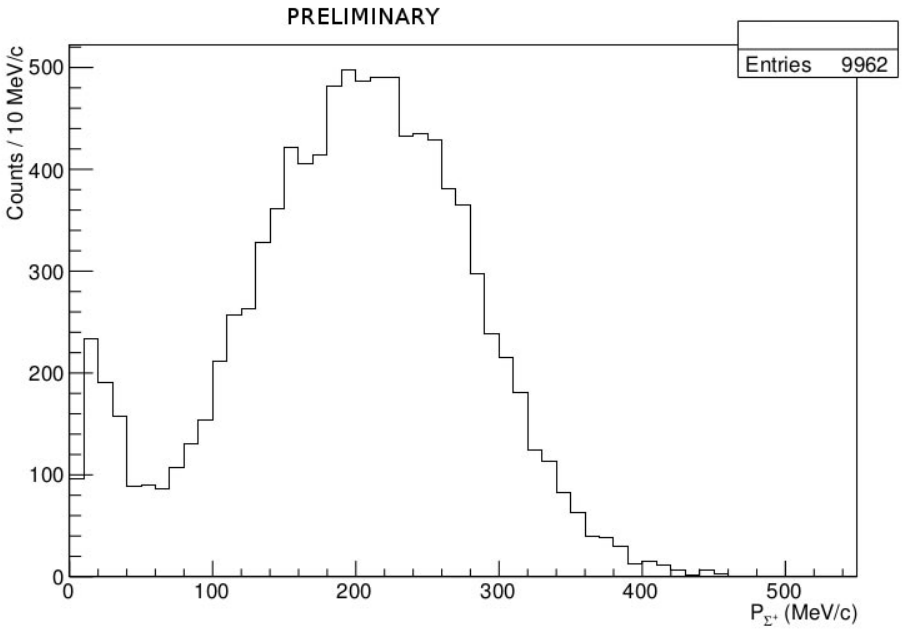

Figure 4. Σ^+ *momentum distribution, from* K^- *captures in* ^{12}C *giving rise to* $\Sigma^+\pi^-$ *formation.*

5 Yπ resonant and non resonant production and the shape of the $\Lambda(1405)$

The position of the $\Lambda(1405)$ state is determined by the strength of the $\bar{K}N$ attractive interaction, and influences the possibility for $\bar{K}$ multi-N formation. When extracting the $\Lambda(1405)$ shape from K^- induced reactions in light nuclear targets (see for example [23]) the hyperon-pion spectroscopy is influenced by the energy threshold, imposed by the last nucleon binding energy. The $m_{\Sigma\pi}$ invariant mass threshold is about 1412 MeV and 1416 MeV, for K^- capture at-rest in Helium and Carbon respectively, thus the K^- absorption at-rest is not sensitive to the high mass pole predicted by chiral unitary models. The $\bar{K}N$ sub-threshold region is accessible by exploiting K^-N absorptions in-flight. For a mean kaon momentum of 100 MeV/c the $m_{\Sigma\pi}$ threshold is shifted upwards of about 10 MeV. A second bias is represented by the non-resonant $K^-N \rightarrow Y\pi$ formation, which gives rise to highly correlated hyperon pion pairs, with narrow (of the order of 10 MeV) $m_{Y\pi}$ invariant masses spectra peaked just below the threshold. The $\Lambda\pi$ and $\Sigma\pi$ non resonant production, for K^- capture in light nuclear targets was never measured. The Λ and π^- kinematic distributions for K^- captures in ^{4}He, both at-rest and in-flight, were calculated in [22]. The momentum probability distribution functions, of the emerging hyperon pion pairs, following K^-n absorptions, are expressed in terms of the K^-n transition amplitudes: the isospin $I = 1$ S-wave non- resonant amplitude ($|f^{nr}|$) and the resonant $I = 1$ P-wave amplitude, dominated by the $\Sigma^-(1385)$. The resonant amplitude is well known from direct experiments, so that measured total momentum distributions can be used to extract the non-resonant $|f^{nr}|$ amplitude module below the $\bar{K}N$ threshold. The goal of the ongoing analyses is to measure the contribution and the shape of the non resonant $\Lambda\pi$ and $\Sigma\pi$ productions. The knowledge of the $(\Sigma\pi)^0$ isospin $I = 0$ non-resonant transition amplitude will allow to disentangle the resonant $\Lambda(1405)$ shape. Preliminary $\Sigma^+\pi^-$ invariant mass spectra, not background subtracted nor acceptance corrected, are

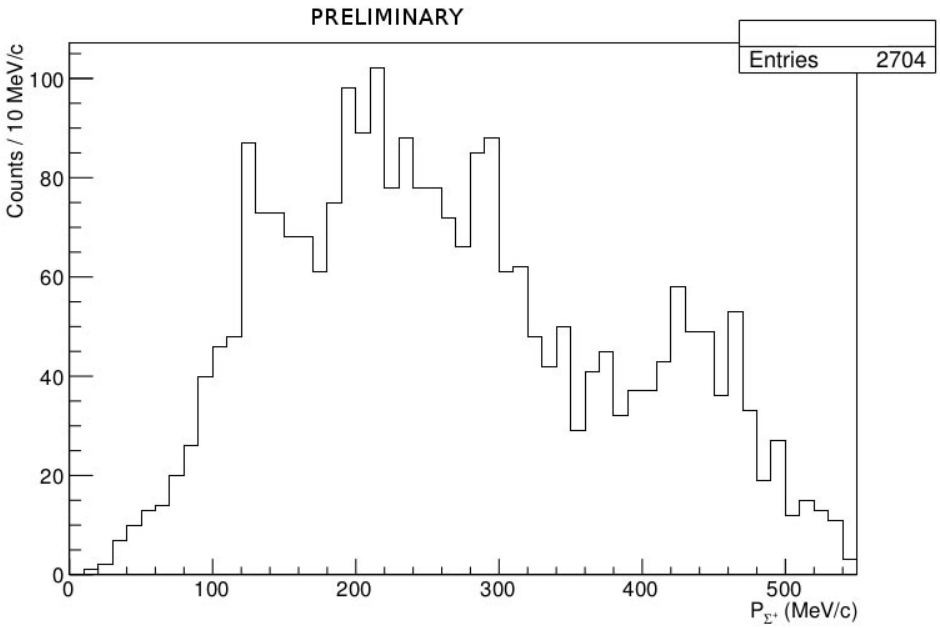

Figure 5. Σ^+ *momentum distribution, from* K^- *captures in* ^{9}*Be giving rise to* $\Sigma^+\pi^-$ *formation.*

shown in Fig. 3. The red curve refers to K^- absorptions on Hydrogen, green and violet distributions refer to K^- captures in-flight and at-rest in ^{12}C respectively, the blue line is the sum of green and violet distributions.

It is also interesting to look at the corresponding distributions of Σ^+ momenta p_{Σ^+} for correlated $\Sigma^+\pi^-$ events. The p_{Σ^+} distributions are shown in Figs. 4 and 5, for K^- captures in ^{12}C (from the KLOE DC entrance wall) and ^{9}Be (from the DAΦNE beryllium sphere) respectively. Figures 4 and 5 can be compared with the corresponding p_{Σ^+} momentum distribution reported by the FINUDA collaboration [24] in Fig. 5 right, this corresponds to K^- captures at-rest on a target of ^{6}Li, producing $\Sigma^+\pi^-$ correlated events. FINUDA data presents a double peak structure, with a low momentum, narrow distribution centered around 20 MeV and a broader bump around 200 MeV. Similar structures can be also recognized in the KLOE data, for K^- captures in ^{12}C (Fig. 4), which is a mixture of K^- absorptions at-rest and in-flight, with different yields of the two peaks. The low momentum peack is not observed in KLOE data for K^- captures in ^{9}Be. Further investigation is needed to understand these interesting features

Acknowledgement

We acknowledge the KLOE Collaboration for their support and for having provided us the data and the tools to perform the analysis presented in this paper.

References

[1] C. Curceanu, K. Piscicchia et al., Acta Phys. Polon. B46 1, 203-215, (2015).

[2] R. Baldini et al., Proposal for a Phi-Factory, report LNF-90/031(R) (1990).
[3] F. Bossi, E. De Lucia, J. Lee-Franzini, S. Miscetti, M. Palutan and KLOE coll., Riv. Nuovo Cim. 31 (2008) 531-623
[4] C. Patrignani et al. (Particle Data Group), Chin. Phys. C, 40, 100001 (2016).
[5] T. Hyodo, D. Jido, Prog. Part. Nucl. Phys. 67 (2012) 55.
[6] Phys. Lett. B 500 (2001),
Phys. Rev. C 66 (2002),
Nucl. Phys. A 725 (2003),
Nucl. Phys. A881, 98 (2012)
[7] T. Yamazaki, *et al.*, Phys. Rev. C **76** 045201 (2007)
A. Doté, *et al.*, Phys. Rev. C **79** 014003 (2009)
S. Wycech, *et al.*, Phys. Rev. C **79** 014001 (2009)
N. Barnea, *et al.*, Phys. Lett. B **712** 132 (2012)
N.V. Shevchenko, *et al.*, Phys. Rev. Lett. **98** 082301 (2007)
Y. Ikeda, *et al.*, Phys. Rev. C **79** 035201 (2009)
E. Oset, *et al.*, Nucl. Phys. A **881** 127 (2012)
[8] G. Agakishiev, *et al.*, HADES Coll., Phys. Lett. B **742** 242 (2015)
[9] M. Agnello, *et al. (FINUDA Coll.)*, Phys. Rev. Lett. **94** 212303 (2005)
[10] T. Yamazaki, *et al.*, Phys. Rev. Lett. **104** 132502 (2010)
[11] Y. Ichikawa, *et al.*, Prog. Theor. Exp. Phys. **021D01** (2015)
[12] A. O. Tokiyasu *et al.*, Phys.Lett. B **728**, 616 (2014)
[13] L. Fabbietti *et al.*, Nucl. Phys. A **914**, 60 (2013)
[14] T. Hashimoto *et al.*, Prog. Theor. Exp. Phys. 061D01 (2015)
[15] K. Piscicchia et al., PoS Bormio2013 034 (2013)
[16] A. Scordo et al., PoS Bormio2014 039 (2014)
[17] M. Adinolfi et al., [KLOE Collaboration], Nucl. Inst. Meth. A 488, (2002) 51.
[18] M. Adinolfi et al. [KLOE Collaboration], Nucl. Inst. Meth. A 482, (2002) 368.
[19] O. Vazquez Doce et al., Phys. Lett. B 758, 134-139 (2016)
[20] R. Roosen, J. H. Wickens, Il Nuovo Cim. A Series 11, **66** 101 (1981)
[21] FINUDA collaboration, Phys. Lett. B, **669** 229 (2008)
[22] K. Piscicchia, S. Wycech, C. Curceanu, Nucl. Phys. A **954**, 75-93 (2016)
[23] J. Esmaili et al., Phys. Lett. B 686 (2010) 23-28
[24] FINUDA collaboration, Phys. Lett. B 704, 474–480 (2011)